

# Electron-impact ionization of $\text{Li}_2$ and $\text{Li}_2^+$

M. S. Pindzola and F. Robicheaux

*Department of Physics, Auburn University, Auburn, Alabama 36849, USA*

C. P. Ballance

*Department of Physics, Rollins College, Winter Park, Florida 32789, USA*

J. Colgan

*Theoretical Division, Los Alamos National Laboratory, Los Alamos, New Mexico 87545, USA*

(Received 20 August 2008; published 15 October 2008)

Electron-impact ionization cross sections for  $\text{Li}_2$  and  $\text{Li}_2^+$  are calculated using a configuration-average distorted-wave method. Bound orbitals for the molecule and its ions are calculated using a single-configuration self-consistent-field method based on a linear combination of Slater-type orbitals. The bound orbitals are transformed onto a two-dimensional lattice  $(r, \theta)$ , which is variable in the radial coordinate and constant in the angular coordinate, from which Hartree with local exchange potentials are constructed. The single-particle Schrödinger equation is then solved for continuum distorted waves with  $S$ -matrix boundary conditions. Total ionization cross sections for  $\text{Li}_2$  at an equilibrium internuclear separation of  $R=5.0$  a.u. and for  $\text{Li}_2^+$  at an equilibrium internuclear separation of  $R=5.9$  a.u. are presented.

DOI: [10.1103/PhysRevA.78.042703](https://doi.org/10.1103/PhysRevA.78.042703)

PACS number(s): 34.50.Gb

## I. INTRODUCTION

An important dynamical process in the understanding of many astrophysical and laboratory plasmas is the electron-impact ionization of atoms or molecules. A reasonably accurate method for calculating the total ionization cross section for atoms and their ions is based on first-order perturbation theory and the use of continuum distorted waves [1]. In the last few years the configuration-average distorted-wave (CADW) method [2] has been used to generate total ionization cross sections and temperature-dependent rate coefficients for all atomic ion stages in the Kr [3] and W [4] isonuclear sequences, as well as both ionization and recombination cross sections and rates for all ion stages in the Ar [5] isonuclear sequence.

Recently, the configuration-average distorted-wave method was extended to enable the generation of total ionization cross sections for diatomic molecules and their ions [6,7]. A key development in the second paper [7] was the extension of the solution of the distorted-wave equations to include  $S$ -matrix boundary conditions. Thus, proper  $l$  mixing is included in the distorted waves for any choice of box radius, solving a long-standing numerical problem [8]. Although CADW ionization cross sections for  $\text{H}_2^+$  were changed very little, the CADW ionization cross sections for  $\text{H}_2$  were reduced by almost 40%. For  $\text{H}_2^+$  and  $\text{H}_2$  the CADW ionization cross sections are now found to be 20–30% above nonperturbative time-dependent close-coupling [9,10] and  $R$  matrix with pseudostates [11] calculations. The very computationally demanding nonperturbative ionization cross section calculations for  $\text{H}_2^+$  and  $\text{H}_2$  are in excellent agreement with experiments [12,13].

In this paper, we further modify the configuration-average distorted-wave method for diatomic molecules to include a variable mesh in the radial coordinate, while keeping the angular coordinate on a constant mesh. A variable radial

mesh makes it easier to handle diatomic molecules with large internuclear separations. We then apply the new CADW method to calculate total ionization cross sections for  $\text{Li}_2$  at an equilibrium internuclear separation of  $R=5.0$  a.u. [14] and for  $\text{Li}_2^+$  at an equilibrium internuclear separation of  $R=5.9$  a.u. [15]. A current application of accurate electron-impact ionization cross sections and rates for Li atoms, molecules, and their ions is found in edge plasma studies of flowing liquid divertor walls [16]. In Sec. II we review the CADW cross section expressions and present the modifications needed for a radial variable mesh, in Sec. III we present ionization cross section results for  $\text{Li}_2$  and  $\text{Li}_2^+$ , and in Sec. IV we give a brief summary. Unless otherwise stated, all quantities are given in atomic units.

## II. THEORY

### A. Cross sections

The most general ionizing transition between configurations of a diatomic molecule is of the form

$$(nl\lambda)^w \epsilon_i l_i \lambda_i \rightarrow (nl\lambda)^{w-1} \epsilon_e l_e \lambda_e \epsilon_f l_f \lambda_f, \quad (1)$$

where  $w$  is the occupation number and  $nl\lambda$ ,  $\epsilon_i l_i \lambda_i$ ,  $\epsilon_e l_e \lambda_e$ , and  $\epsilon_f l_f \lambda_f$  are the quantum numbers of the bound valence electron and the incident, ejected, and final continuum electrons ( $\lambda=|m|$  is the absolute value of the magnetic quantum number).

The configuration-average ionization cross section is given by

$$\sigma_{\text{ion}} = \int_0^{E/2} d\epsilon_e \frac{64}{k_i^3 k_e k_f} \frac{w}{S(\lambda)} \sum_{l_i, \lambda_i} \sum_{l_e, \lambda_e} \sum_{l_f} (M_d + M_e - M_x), \quad (2)$$

where the total energy  $E = \epsilon_{nl\lambda} + \epsilon_i = \epsilon_e + \epsilon_f$ ,  $\epsilon = k^2/2$ ,  $S(\lambda) = 2(2 - \delta_{\lambda,0})$  is the statistical weight of the  $nl\lambda$  orbital, and the

continuum normalization is chosen as one times a sine function. The direct  $M_d$ , exchange  $M_e$ , and cross  $M_x$  terms may be expressed in terms of weighted sums over polar coordinate Coulomb integrals [6,7]. The bound and continuum reduced orbitals  $u(r, \theta)$  found in the Coulomb integrals are defined by

$$\psi(r, \theta, \phi) = \frac{u(r, \theta) e^{im\phi}}{r\sqrt{\sin \theta} \sqrt{2\pi}}, \quad (3)$$

where  $\psi(r, \theta, \phi)$  is the spatial part of the single-particle wave function and the bound normalization is  $\int_0^\infty dr \int_0^\pi d\theta [u(r, \theta)]^2 = 1$ .

### B. Bound orbitals and potentials

The bound orbitals for the molecule and its ions are calculated using a single-configuration self-consistent-field method based on a linear combination of Slater-type orbitals [17]. The molecular bound orbitals are then transformed [18] onto a two-dimensional  $(r, \theta)$  numerical lattice to yield bound reduced orbitals  $u_{n\lambda}(r, \theta)$ . The radial coordinate is discretized on a variable mesh:

$$r_{i+1} = \begin{cases} r_i + \Delta r_{\min} + i \delta r & \text{for } 0 < r_i < r_{\text{cut}}, \\ r_i + \Delta r_{\max} & \text{for } r_{\text{cut}} < r_i < r_{\text{final}}, \end{cases} \quad (4)$$

while the angular coordinate is discretized on a constant mesh:

$$\theta_{i+1} = \theta_i + \Delta \theta. \quad (5)$$

Using the molecular bound orbitals we construct a Hartree with local exchange potential:

$$V_{\text{HX}}(r, \theta) = V_{\text{direct}}(r, \theta) + V_{\text{exchange}}(r, \theta). \quad (6)$$

The direct potential is given by

$$V_{\text{direct}}(r, \theta) = \sum_k v_k(r) P_0^k(\cos \theta), \quad (7)$$

where  $P_m^l(\cos \theta)$  is an associated Legendre polynomial and

$$v_k(r) = \sum_{n\lambda} w_{n\lambda} \int_0^\infty dr' \int_0^\pi d\theta' [u_{n\lambda}(r', \theta')]^2 \frac{r^k}{r'^{k+1}} P_0^k(\cos \theta'), \quad (8)$$

while the local exchange potential is given by

$$V_{\text{exchange}}(r, \theta) = -\frac{1}{2} \left( \frac{24\rho(r, \theta)}{\pi} \right)^{1/3}, \quad (9)$$

where

$$\rho(r, \theta) = \sum_{n\lambda} w_{n\lambda} \frac{[u_{n\lambda}(r, \theta)]^2}{2\pi r^2 \sin \theta}. \quad (10)$$

### C. Continuum orbitals

The distorted-wave continuum orbitals are found by the solution of the single-particle Schrödinger equation:

$$\left( -\frac{1}{2} \nabla^2 + V_{\text{nuclear}}(r, \theta) + V_{\text{HX}}(r, \theta) - \epsilon \right) \psi(r, \theta, \phi) = 0, \quad (11)$$

where the nuclear potential is given by

$$V_{\text{nuclear}}(r, \theta) = -\frac{Z}{\sqrt{r^2 + \frac{1}{4}R^2 - rR \cos \theta}} - \frac{Z}{\sqrt{r^2 + \frac{1}{4}R^2 + rR \cos \theta}}, \quad (12)$$

$Z$  is the charge on each nucleus of a homonuclear diatomic molecule, and  $R$  is the internuclear separation distance. The variational principle applied to the single-particle Schrödinger equation on a two-dimensional  $(r, \theta)$  numerical lattice, which is variable in the radial coordinate and constant in the angular coordinate, yields

$$(K + V_{\text{centrifugal}} + V_{\text{nuclear}} + V_{\text{HX}} - \epsilon)u(r_i, \theta_j) = 0, \quad (13)$$

where the kinetic energy operator is given by

$$Ku(r_i, \theta_j) = -[c_i^+ u(r_{i+1}, \theta_j) + c_i^- u(r_{i-1}, \theta_j) - c_i^0 u(r_i, \theta_j)] - \frac{1}{2r_i^2 \Delta \theta^2} [d_j^+ u(r_i, \theta_{j+1}) + d_j^- u(r_i, \theta_{j-1}) - d_j^0 u(r_i, \theta_j)], \quad (14)$$

and the centrifugal potential is given by

$$V_{\text{centrifugal}}(r, \theta) = \frac{\lambda^2}{2r^2 \sin^2 \theta}. \quad (15)$$

The variational coefficients in the kinetic energy operator are given by

$$c_i^+ = \frac{r_{i+1/2}^2}{r_i r_{i+1} (r_{i+1} - r_{i-1}) (r_{i+1} - r_i)}, \quad (16)$$

$$c_i^- = \frac{r_{i-1/2}^2}{r_i r_{i-1} (r_{i+1} - r_{i-1}) (r_i - r_{i-1})}, \quad (17)$$

$$c_i^0 = \frac{r_{i+1/2}^2}{r_i^2 (r_{i+1} - r_{i-1}) (r_{i+1} - r_i)} + \frac{r_{i-1/2}^2}{r_i^2 (r_{i+1} - r_{i-1}) (r_i - r_{i-1})}, \quad (18)$$

$$d_j^+ = \frac{\sin \theta_{j+1/2}}{\sqrt{\sin \theta_j \sin \theta_{j+1}}}, \quad (19)$$

$$d_j^- = \frac{\sin \theta_{j-1/2}}{\sqrt{\sin \theta_j \sin \theta_{j-1}}}, \quad (20)$$

$$d_j^0 = \frac{\sin \theta_{j+1/2}}{\sin \theta_j} + \frac{\sin \theta_{j-1/2}}{\sin \theta_j}. \quad (21)$$

Following standard Wentzer–Kramers–Brillouin (WKB) theory, we choose  $S$ -matrix boundary conditions with long-

range unit normalization for the continuum orbitals. We solve Eq. (13) including  $S$ -matrix boundary conditions as a system of linear equations  $\mathbf{A}\mathbf{u}=\mathbf{b}$ . A key element in guarding against  $l$  mixing in the continuum orbitals is to solve for the normalized associated Legendre functions found in the  $S$ -matrix boundary conditions by matrix diagonalization of the angular part of the single-particle Schrödinger equation [7].

### III. RESULTS

The configuration-average distorted-wave method is used to calculate the electron-impact single-ionization cross section for  $\text{Li}_2$  at an equilibrium internuclear separation of  $R=5.0$  a.u. [14] and for  $\text{Li}_2^+$  at an equilibrium internuclear separation of  $R=5.9$  a.u. [15]. We employ a  $(5000 \times 64)$ -point lattice in  $(r, \theta)$  spherical polar coordinates. The variable radial mesh begins with  $\Delta r_{\min}=0.10$ , changes by  $\delta r=0.001$  until  $r_{\text{cut}}=40.0$ , and then uses a constant  $\Delta r_{\max}=0.30$  until  $r_{\text{final}}=1480.0$ . The constant angular mesh uses  $\Delta\theta=0.015\ 625\pi$ .

Single-configuration calculations [17] yield for  $\text{Li}_2$  ( $R=5.0$ ) a total energy of  $-16.67$  a.u., for  $\text{Li}_2^+$  ( $R=5.0$ ) a total energy of  $-16.51$  a.u., for  $\text{Li}_2^+$  ( $R=5.9$ ) a total energy of  $-16.24$  a.u., and for  $\text{Li}_2^{2+}$  ( $R=5.9$ ) a total energy of  $-15.83$  a.u.. More elaborate calculations using Coulomb and polarization model potentials yield more accurate total energies [15]. The bound orbitals are then transformed [18] onto the two-dimensional  $(r, \theta)$  lattice. The direct and exchange potentials for ionization of the  $2\sigma_g$  orbital of  $\text{Li}_2$  ( $R=5.0$ ) are calculated using Eqs. (6)–(10) and the  $1\sigma_g$ ,  $1\sigma_u$ , and  $2\sigma_g$  orbitals of  $\text{Li}_2^+$  ( $R=5.0$ ). The scattering potentials for ionization of the  $2\sigma_g$  orbital of  $\text{Li}_2^+$  ( $R=5.9$ ) are calculated using the  $1\sigma_g$  and  $1\sigma_u$  orbitals of  $\text{Li}_2^{2+}$  ( $R=5.9$ ).

Partial ionization cross sections are calculated using Eq. (2) for  $l_i=0-9$  and  $\lambda_i=0-4$  and extrapolated to higher  $l_i$  and  $\lambda_i$  using appropriate fitting functions. Numerical implementation of Eq. (2) takes advantage of a simple partition over all  $l_i$ ,  $\lambda_i$ ,  $l_e$ , and  $\lambda_e$  on a massively parallel computer.

Electron-impact ionization cross section results for  $\text{Li}_2$  are presented in Fig. 1. Configuration-average distorted-wave results are presented at  $R=5.0$  a.u. and compared with results using a one-parameter binary encounter Bethe (BEB) method [19], both obtained using an ionization potential of 5.11 eV [20]. For further comparison, since we are not aware of any experimental results, we also present CADW results for electron ionization of two Li atoms, corresponding to  $\text{Li}_2$  as  $R \rightarrow \infty$ , and for electron ionization of the C atom, corresponding to  $\text{Li}_2$  as  $R \rightarrow 0$ . The atomic CADW calculations are carried out for  $l_i=0-50$  and no extrapolations are needed even at the highest incident energies. The good agreement in general shape between the CADW results for electron ionization of  $\text{Li}_2$  at  $R=5.0$  and the CADW results for two Li atoms gives us confidence in the extrapolations used in the molecular CADW calculations. We note that the one-parameter BEB method has been generalized to accurately predict total ionization cross sections for many other molecules and their ions [21].

Electron-impact ionization cross section results for  $\text{Li}_2^+$  are presented in Fig. 2. Configuration-average distorted-

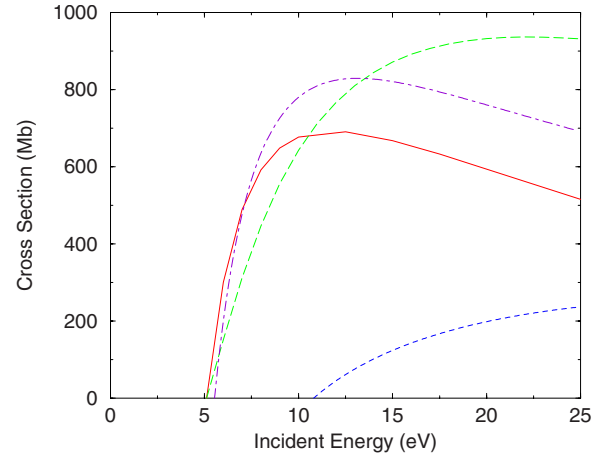


FIG. 1. (Color online) Electron-impact ionization of  $\text{Li}_2$ . Solid line (red), distorted-wave calculation at  $R=5.0$ ; dot-dashed line (purple), distorted-wave calculation for two Li atoms or  $\text{Li}_2$  as  $R \rightarrow \infty$ ; short-dashed line (blue), distorted-wave calculation for a C atom or  $\text{Li}_2$  as  $R \rightarrow 0$ ; long-dashed line (green), BEB calculation. ( $1.0 \text{ Mb}=1.0 \times 10^{-18} \text{ cm}^2$ .)

wave results are presented at  $R=5.9$  a.u. and compared with BEB results, both obtained using an ionization potential of 11.5 eV. For further comparison, since we are not aware of any experimental results, we also present CADW results for electron ionization of the  $\text{C}^+$  atomic ion, corresponding to  $\text{Li}_2^+$  as  $R \rightarrow 0$ .

### IV. SUMMARY

In conclusion, we have extended a configuration-average distorted-wave method to make use of a two-dimensional  $(r, \theta)$  lattice which is variable in the radial coordinate and constant in the angular coordinate. The CADW method was then applied to calculate the electron-impact ionization cross

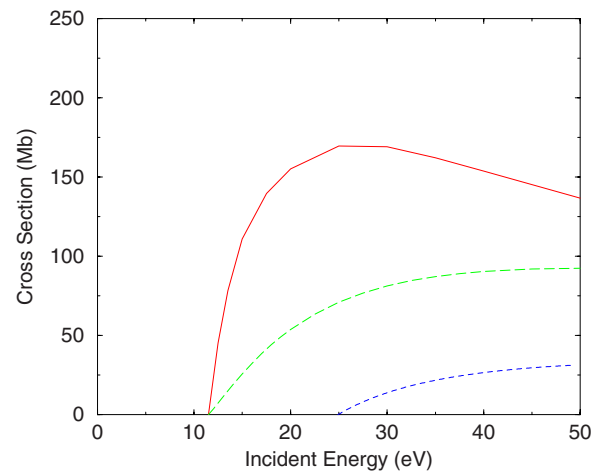


FIG. 2. (Color online) Electron-impact ionization of  $\text{Li}_2^+$ . Solid line (red), distorted-wave calculation at  $R=5.9$ ; short dashed line (blue), distorted-wave calculation for a  $\text{C}^+$  atomic ion or  $\text{Li}_2^+$  as  $R \rightarrow 0$ ; long dashed line (green), BEB calculation. ( $1.0 \text{ Mb}=1.0 \times 10^{-18} \text{ cm}^2$ .)

sections for  $\text{Li}_2$  and  $\text{Li}_2^+$ . Both diatomic molecules have quite large equilibrium internuclear separations.

In the future, we plan to apply the molecular CADW method to calculate electron-impact ionization cross sections for a variety of diatomic molecules and their ions. Previous CADW calculations [6,7] for  $\text{H}_2$  and  $\text{H}_2^+$  have found that the perturbative theoretical results lie between 20% and 30% above experimental results. To further improve the accuracy of theoretical predictions of the electron-impact ionization cross sections for diatomic molecules and their ions, we also plan to extend the time-dependent close-coupling method [9,10] to include a variable radial mesh. Our first application

will be to produce nonperturbative theoretical results for the ionization of  $\text{Li}_2$  and  $\text{Li}_2^+$  to check our perturbative CADW predictions.

#### ACKNOWLEDGMENTS

This work was supported in part by grants from the U.S. Department of Energy. Computational work was carried out at the National Energy Research Scientific Computing Center in Oakland, California and at the National Center for Computational Sciences in Oak Ridge, Tennessee.

- 
- [1] S. M. Younger, *Phys. Rev. A* **22**, 111 (1980).  
[2] M. S. Pindzola, D. C. Griffin, and C. Bottcher, in *Atomic Processes in Electron-Ion and Ion-Ion Collisions*, edited by F. Brouillard, NATO Advanced Study Institute, Series B: Physics (Plenum, New York, 1986), Vol. 145, p. 75.  
[3] S. D. Loch, M. S. Pindzola, C. P. Ballance, D. C. Griffin, D. M. Mitnik, N. R. Badnell, M. G. O'Mullane, H. P. Summers, and A. D. Whiteford, *Phys. Rev. A* **66**, 052708 (2002).  
[4] S. D. Loch, J. A. Ludlow, M. S. Pindzola, A. D. Whiteford, and D. C. Griffin, *Phys. Rev. A* **72**, 052716 (2005).  
[5] S. D. Loch, S. A. Abdel-Naby, C. P. Ballance, and M. S. Pindzola, *Phys. Rev. A* **76**, 022706 (2007).  
[6] M. S. Pindzola, F. Robicheaux, J. A. Ludlow, J. Colgan, and D. C. Griffin, *Phys. Rev. A* **72**, 012716 (2005).  
[7] M. S. Pindzola, F. Robicheaux, J. Colgan, and C. P. Ballance, *Phys. Rev. A* **76**, 012714 (2007).  
[8] J. C. Tully and R. S. Berry, *J. Chem. Phys.* **51**, 2056 (1969).  
[9] M. S. Pindzola, F. Robicheaux, and J. Colgan, *J. Phys. B* **38**, L285 (2005).  
[10] M. S. Pindzola, F. Robicheaux, S. D. Loch, and J. P. Colgan, *Phys. Rev. A* **73**, 052706 (2006).  
[11] J. D. Gorfinkel and J. Tennyson, *J. Phys. B* **38**, 1607 (2005).  
[12] B. Peart and K. T. Dolder, *J. Phys. B* **6**, 2409 (1973).  
[13] H. C. Straub, P. Renault, B. G. Lindsay, K. A. Smith, and R. F. Stebbings, *Phys. Rev. A* **54**, 2146 (1996).  
[14] K. P. Huber and G. Herzberg, *Constants of Diatomic Molecules* (Van Nostrand Reinhold, New York, 1979).  
[15] S. Magnier, S. Rousseau, A. R. Allouche, G. Hadinger, and M. Aubert-Frecon, *Chem. Phys.* **246**, 57 (1999).  
[16] J. N. Brooks and J. P. Allain, *Fusion Sci. Technol.* **47**, 669 (2005).  
[17] Theoretical Chemistry Group, computer code ALCHEMY (IBM Research Laboratory, San Jose, CA, 1970).  
[18] M. A. Morrison, *Comput. Phys. Commun.* **21**, 63 (1980).  
[19] Y. K. Kim and M. E. Rudd, *Phys. Rev. A* **50**, 3954 (1994).  
[20] See <http://physics.nist.gov/PhysRefData>  
[21] W. M. Huo, *Phys. Rev. A* **64**, 042719 (2001).